Scanning tunneling microscopy study of superconductivity, magnetic vortices, and possible charge-density wave in $Ta_4Pd_3Te_{16}$

Q. Fan,[1] W. H. Zhang,[1] X. Liu,[1] Y. J. Yan,[1] M. Q. Ren,[1] M. Xia,[1] H. Y. Chen,[1] D. F. Xu,[1] Z. R. Ye,[1] W. H. Jiao,[2,3] G. H. Cao,[2,3] B. P. Xie,[1,3] T. Zhang,[1,3,*] and D. L. Feng[1,3]

[1]*State Key Laboratory of Surface Physics, Department of Physics, and Advanced Materials Laboratory, Fudan University, Shanghai 200433, China*

[2]*Department of Physics, Zhejiang University, Hangzhou 310027, China*

[3]*Collaborative Innovation Center of Advanced Microstructures, Nanjing 210093, P. R. China*

(Received 24 December 2014; revised manuscript received 21 February 2015; published 11 March 2015)

$Ta_4Pd_3Te_{16}$ is a newly discovered layered superconductor with quasi-one-dimensional (1D) structure. Recent thermal transport measurements show the possible existence of nodes in the superconducting gap. Here we report low-temperature scanning tunneling microscopy/spectroscopy study on $Ta_4Pd_3Te_{16}$ single crystals. We observed stripelike structure composed of atom chains on the cleaved $(\bar{1}03)$ surface. There exists charge-density-wave (CDW)-like modulations along stripes with commensurate periods. Meanwhile, the tunneling conductance shows an s-wave-like superconducting gap. The magnetic vortex mapped at low field is highly anisotropic with a bound state in the core. At increased field, strong vortex overlapping is directly observed and the bound state is suppressed, indicating the delocalization of the superconducting quasiparticles. Our observations suggest that $Ta_4Pd_3Te_{16}$ is of multiband superconductivity with strong 1D characters, which possibly coexist with CDW transition.

DOI: 10.1103/PhysRevB.91.104506 PACS number(s): 74.55.+v, 74.25.Jb, 74.25.Uv, 74.70.−b

Superconductivity in low-dimensional systems has long been a fascinating topic in condensed matter physics. The increased phase fluctuation is an obstacle of electron paring, and unique orders such as charge/spin density waves (CDW/SDW) may also compete with superconductivity. However, for last decades, many superconductors were found at low dimensions. For examples, cuprates [1], iron-based material [2], and heavy fermion materials like $CeCoIn_5$ [3], all have quasi-two-dimensional (2D) structure. They are also believed to be unconventional superconductors. But for the quasi-one-dimensional (1D) case, represented by the compounds $(TMTSF)_2X$ ($X = PF_6$, ClO_4) [4,5] and $Li_{0.9}Mo_6O_{17}$ [6], how the superconductivity would exist and behave is still unclear.

Recently, Jiao *et al.* reported superconductivity in a layered materials $Ta_4Pd_3Te_{16}$ with quasi-1D chains, which has a superconducting transition temperature T_c of 4.6 K [7]. The specific heat measurement suggests that there might be strong electron-electron interactions in this system. Soon after, Pan *et al.* reported thermal conductivity of $Ta_4Pd_3Te_{16}$ measured at temperature down to 80 mK [8], which shows significant residual linear term at zero field and its field dependence resembles that of cuprate superconductors. The band structure calculations show that $Ta_4Pd_3Te_{16}$ is a multiband system, whose low energy electronic structure near the Fermi energy (E_F) is mainly contributed by the Te 5p states with little correlation [9,10]. Thus the thermal transport data might be interpreted by its multiband nature, where the gap of certain band could be very small, rather than by a nodal superconducting gap structure. To clarify these two scenarios, more direct measurements of the superconducting state are required.

In this paper, we report low-temperature scanning tunneling microscope (STM) and spectroscopy (STS) measurements on $Ta_4Pd_3Te_{16}$ single crystals. The surface atomic structure, superconducting gap, and magnetic vortex states are investigated. We observed commensurate modulations along atom chains of the $(\bar{1}03)$ surface, which might arise from a CDW. At 0.4 K, the tunneling conductance around E_F shows a BCS-like gap, which is inconsistent with the presence of nodes. Single magnetic vortex mapped at low field is highly anisotropic, with the size much larger than the value expected from its upper critical field (H_{c2}), and a zero bias bound state is observed in the core. Interestingly, when the field increases, the vortex core size "shrinks" significantly and the core bound states are also quickly suppressed. By referring to the band calculations in Ref. [9], our observations can be understood in the framework of multiband superconductivity. The anomalous field dependence of vortices implies there should exist a "hidden" band (overwhelmed by others in the tunneling conductance) with shorter coherence length and larger superconducting gap, which likely dominates samples bulk superconductivity. Thus $Ta_4Pd_3Te_{16}$ provides a novel platform to study the interplay between quasi-1D superconductivity, multiband effect, and possible CDW instabilities.

The experiment was conducted in a commercial STM (Unisoku) with a base temperature of 0.4 K. $Ta_4Pd_3Te_{16}$ single crystals were grown by self-flux method [7] with $T_c \approx 4.3$ K and a H_{c2} of 2.9 T along c' axis [8] (c' axis is along $[\bar{1}03]$ direction). We cleaved the sample in ultrahigh vacuum (1×10^{-10} torr) before transferring into STM module. Normal PtIr tips were cleaned by e-beam heating before the measurement. The topographic images are taken with constant current mode, and the tunneling conductance dI/dV is collected by standard lock-in method with a modulation frequency of 973 Hz.

Figure 1(a) shows the typical topography of the cleaved surface, corresponding to the $(\bar{1}03)$ plane of $Ta_4Pd_3Te_{16}$. The surface is atomically flat, featured by regular stripes with a spacing of 2.7 nm. By zooming into a $5 \times 5\,nm^2$ region

*tzhang18@fudan.edu.cn

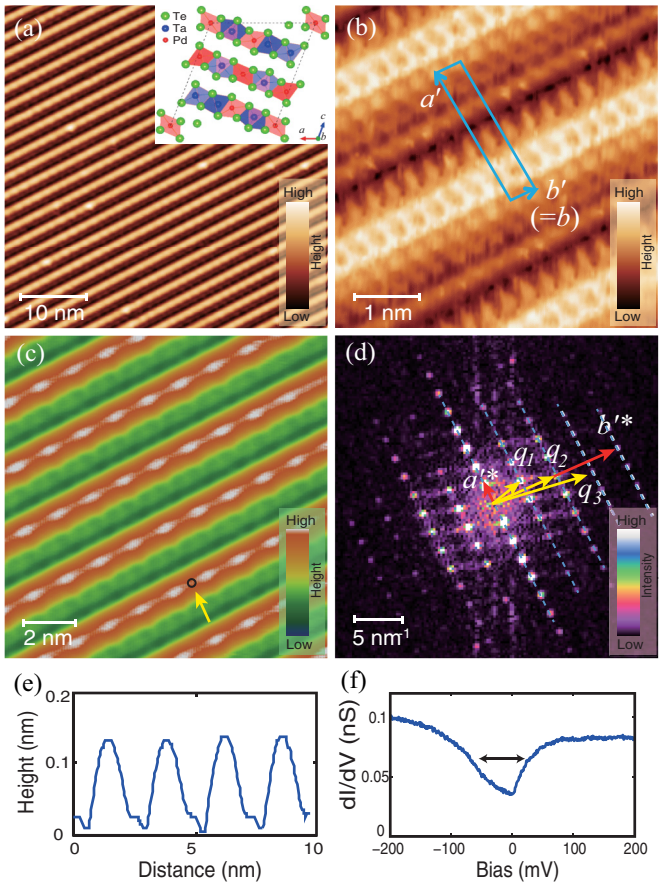

FIG. 1. (Color online) STM topography of $Ta_4Pd_3Te_{16}$ and CDW-like modulations. (a) 50 nm × 50 nm STM image (V_{bias} = 1.0 V, I = 30 pA). Insert: Crystal structure of $Ta_4Pd_3Te_{16}$ projected along the [010] directions. (b) Atomically resolved STM image (5 nm × 5 nm, V_{bias} = 10 meV, I = 50 pA). (c) STM image showing additional modulations (12 nm × 12 nm, $V_{bias} = -100$ meV, I = 50 pA). The yellow arrow points to the location where the spectrum in (f) was taken. (d) The Fourier transformation of (c). Lattice Bragg spots are marked by $\mathbf{a}'^*$ and $\mathbf{b}'^*$. Wave vectors of additional modulations are marked by $\mathbf{q}_1$, $\mathbf{q}_2$, $\mathbf{q}_3$. (e) A line profile taken in (a), which shows the surface corrugation. (f) dI/dV spectrum measured at the position shown in (c) at 4 K, within the bias range of −200 meV ∼200 meV.

[Fig. 1(b)], the lattice with atom chains can be seen. The surface unit cell marked in Fig. 1(b) has the in-plane constants of $a' = 28$ Å, $b'(= b) = 3.7$ Å, agree with the x-ray data [7,11]. According to the crystal structure of $Ta_4Pd_3Te_{16}$ [as shown in the insert of Fig. 1(a)], the $(\bar{1}03)$ plane is composed of alternatively arranged $PdTe_2$, $TaTe_3$, and Ta_2Te_4 chains [11]. The brightest double chain in the image is likely to be the Ta_2Te_4 chains. As shown in Fig. 1(e), the apparent corrugation of different chains is about 1.4 Å, which is much larger than the lattice corrugation itself (∼0.1 Å) [9]. This large corrugation shall be due to unevenly distributed local density of states (LDOS), which is a signature of quasi-1D structure.

Besides the stripelike surface structure, additional weak modulations on the surface are found. Figure 1(c) is an STM image taken at 4 K with $V_{bias} = -100$ meV, a modulation with a period of $4\mathbf{b}'$ along the bright stripe is clearly visible, and some weaker ones in the dim area can also be seen (images taken at 0.4 K also show the same modulations). The corrugations of these modulations are less than 0.05 Å. To identify them clearly, we make the 2D Fourier transformation of Fig. 1(c), as shown in Fig. 1(d). The lattice Bragg spots marked by $\mathbf{a}'^*$ and $\mathbf{b}'^*$ and their harmonics are visible. Three sets of additional modulation vectors ($\mathbf{q}_1$, $\mathbf{q}_2$, $\mathbf{q}_3$) are found as satellite spots in between the Bragg spots. Their equal spacing in $\mathbf{b}'^*$ direction (shown by dashed line) indicates they have exact periods of $4b'$, $2b'$, $4/3b'$ along $\mathbf{b}'$, respectively. Considering the quasi-1D structure of $Ta_4Pd_3Te_{16}$, these along-chain modulations are possibly from Peierls (CDW) transition. Similar modulations have been observed in typical 1D CDW material, such as TTF-TCNQ [12] and $NbSe_3$ [13]. But the coexistence of CDW and superconductivity in quasi-1D systems is rare, although the coexistence of CDW and superconductivity is common in 2D systems such as the transition metal chalcogenides. In Fig. 1(f), we show the tunneling spectrum measured at 4 K with the large bias range of −200 meV ∼200 meV, a gaplike structure with finite conductance inside is observed, which might be due to CDW transition. We noticed the CDW is also predicted in Ref. [9], but here the commensurate periods differ from the calculations.

Now we turn to superconductivity measurement. Figure 2(a) shows the tunneling conductance measured at 0.4 K within ±3 mV around E_F. A well-defined superconducting gap with coherence peaks is observed, and the tunneling conductance in the gap bottom reaches zero. The gap is found to be spatially homogenous. In Figs. 2(b) and 2(c) we show the spectra measured at two different locations, one on the bright stripe and one between stripes, no significant difference of the spectra can be observed. The tunneling spectrum can be basically fitted into a single BCS gap formula: $N(E) = \mathrm{Re}(|E|/\sqrt{E^2 - \Delta^2})$, with broadenings due to thermal, electronic noises, and finite quasiparticle lifetime. Here we use an effective temperature (T_{eff}) to account for all the broadening factors. The fitting [black curve in Fig. 2(a)] yields $\Delta = 0.66$ meV ($\sim 1.78 k_B T_c$) and $T_{\mathrm{eff}} = 1.2$ K. Since the broadening will strongly affect the measured gap line shape, we checked the superconducting gap of Pb with the same tip right after this experiment, and obtained the same T_{eff} of 1.2 K [Fig. 2(a) insert]. The BCS-like gap indicates $Ta_4Pd_3Te_{16}$ is an s-wave superconductor. For comparison we draw a d-wave gap with similar gap size ($\Delta = \Delta_0 \cos(2\theta)$) and T_{eff} in Fig. 2(a) (the blue dashed curve), it clearly deviates from our data. One may further argue that the data slightly deviate from the single-gap BCS fitting. However, since $Ta_4Pd_3Te_{16}$ is predicted to be a multiband system [9], the deviation could be due to multigap contributions, or gap anisotropy, which can be well expected for this anisotropic material. However, high-resolution and low-temperature angle resolved photoemission spectroscopy (ARPES) measurement is needed to clarify these.

To further inspect the superconductivity of $Ta_4Pd_3Te_{16}$, we applied magnetic field perpendicular to the sample surface (i.e., along the c' axis). For type II superconductors the field will penetrate into the bulk in the form of quantized vortices. Figures 3(a)–3(h) show the zero bias conductance (ZBC) mappings measured at 0.4 K at different fields, in a 200 × 200 nm^2 area (ZBC values are all normalized by the

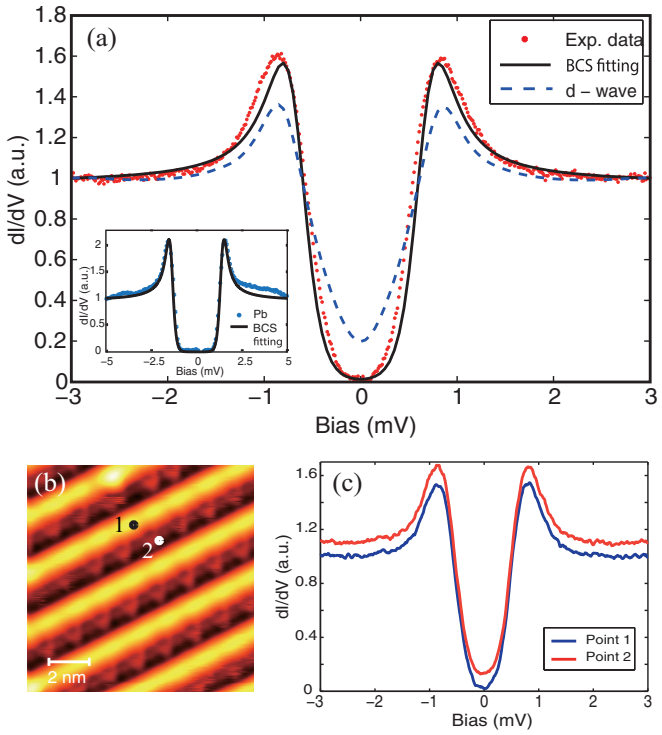

FIG. 2. (Color online) The superconducting gap spectrum of $Ta_4Pd_3Te_{16}$ and its spatial homogeneity. (a) Red spots: Normalized dI/dV spectrum taken at 0.4 K with a modulation of 50 μeV. Black solid curve: BCS fitting with $\Delta = 0.66$ meV and $T_{\rm eff} = 1.2$ K. Blue dashed line: simulated d-wave curve using $\Delta = \Delta_0 \cos(2\theta)$ with $\Delta_0 = 0.8$ meV and $T_{\rm eff} = 1.2$ K. (Insert: dI/dV spectrum taken on Pb film at 0.4 K, the black solid curve is BCS fitting with $\Delta = 1.39$ meV and $T_{\rm eff} = 1.2$ K) (b) A 10 nm $\times$ 10 nm STM image showing the positions for the measured spectra in (c). (c) dI/dV spectra taken on the two points marked in (b). The red curve is shifted up for clarification.

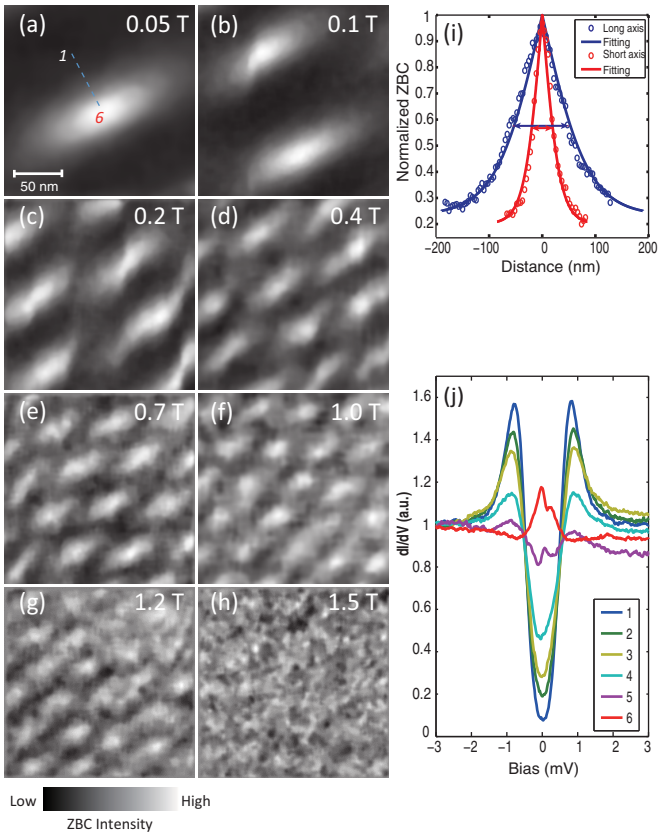

FIG. 3. (Color online) Magnetic vortex imaging of $Ta_4Pd_3Te_{16}$ and the vortex core bound states. (a)–(h) Zero bias conductance (dI/dV) mappings measured at 0.4 K at different fields (labeled in the mapping), taken in a same area of 200 nm $\times$ 200 nm. Scale bar is marked in (a). (i) Line profiles of the vortex core in (a), taken along the long axis (blue spots) and short axis (red spots). Solid curves are fittings by using Eq. (1), which yield $\xi_{b'} = 105$ nm, $\xi_{a'} = 36$ nm. Arrows show the FWHMs of the vortex core along long and short axes. (j) dI/dV spectra taken along the dashed line (points 1 to 6) in (a). At the center of the vortex core (on point 6), a zero bias peak is observed (the red curve).

conductance at the $V_{\rm bias}$ of -3 meV through the whole paper). The emergence of vortices is clearly seen (high ZBC regions correspond to vortex cores). First we focus on the single vortex measured at the low field of 0.05 T in Fig. 3(a). It is elliptical shaped, with the ratio of long axis to short axis about 3:1. The elongated direction is parallel to the atom chains. Figure 3(j) shows the spectra measured along the dashed line in Fig. 3(a). As moving to the core, the superconducting gap is gradually suppressed and a zero bias bound state is observed at the core center. The core bound state is well expected for a clean s-wave superconductor in isolated vortices, which is caused by Andreev scatterings of the confined quasiparticles [14,15]. In general, the size and shape of a vortex core is determined by coherence length (ξ). In BCS theory $\xi_{\rm BCS} = h v_F/\pi\Delta$, one can expect the electrons with k parallel to the chains will be more mobile, with larger v_F and thus longer $\xi_{\rm BCS}$ along the chains. Band calculations also show the Fermi surfaces of $Ta_4Pd_3Te_{16}$ are highly anisotropic for all the bands across E_F [9]. Thus the observed anisotropy is another manifestation of quasi-1D structure. Considering the averaged spacing between vortices at 0.05 T will be 220 nm, the vortex in Fig. 3(a) is nearly isolated. We can estimate the GL coherence length (ξ_{GL}) by fitting the GL expression of the order parameter:

$$f(r) = \tanh(r/\sqrt{2}\xi_{GL}) = 1 - \sigma(r,0) \qquad (1)$$

where $\sigma(r,0)$ is the normalized ZBC at the distance r to the core center, and $1-\sigma$ is proportional to the order parameter. The fitted value along the long and short axis ($\xi_{b'} = 105$ and $\xi_{a'} = 36$ nm, respectively) produces an averaged $\overline{\xi_{GL}} = \sqrt{\xi_{a'}\xi_{b'}} = 61$ nm [fitting is shown in Fig. 3(i)]. Note that for a usual type-II superconductors, ξ_{GL} relates to the upper critical field by $H_{c2} = \varphi_0/2\pi\xi_{GL}^2$. The bulk H_{c2} of $Ta_4Pd_3Te_{16}$ along the c' axis is 2.9 T, which gives a $\xi_{GL}(H_{c2})$ of only 11 nm. This big discrepancy is clearly anomalous for normal type-II superconductors. It implies the observed gap may not be the one that dominates the H_{c2} of $Ta_4Pd_3Te_{16}$, which is an evidence of the multiband superconductivity in this material [16,17].

To further explore the vortex properties, mappings at increased field are carried out, as shown in Figs. 3(b)–3(h). A remarkable feature is that the core size seems to "shrink" rapidly with increasing field. At the same time, the

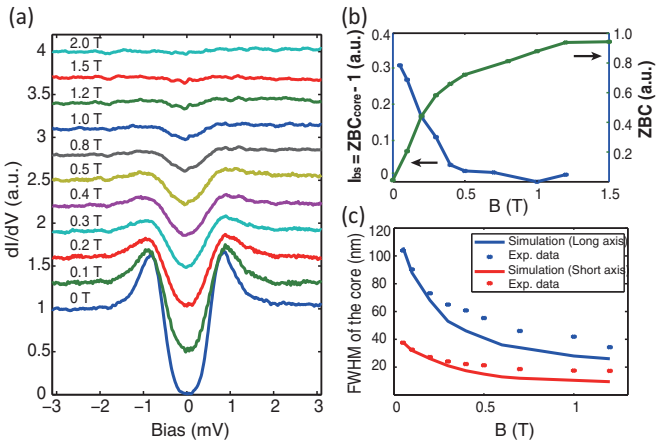

FIG. 4. (Color online) Field dependence of the superconducting properties. (a) dI/dV spectrum measured in the middle point between two vortices (along the short axis) at various magnetic fields. (b) Left axis (blue curve): the strength of vortex core bound state (defined by $I_{bs} = \mathrm{ZBC_{core}} - 1$) that measured at the core center, as a function of field. Right axis (green curve) ZBC values extracted from (a), as a function of field. (c) The FWHMs of the vortex cores measured along long axis (blue spots) and short axis (red spots),as the function of field. The solid curves are calculated from the vortex overlapping model (Ref. [17]).

superconducting gap measured outside of the vortices (at the middle point between two vortices) was rapidly suppressed by the field, as shown in Figs. 4(a) and 4(b) (the ZBC is quickly enhanced by the magnetic field). At $B = 1.5$ T, the superconducting gap is completely disappeared across the sample and vortex lattice also can no longer be resolved, but this field is still far below the H_{c2} of 2.9 T. Moreover, the core bound state observed in Fig. 3(j) is also quickly suppressed by the field. In Fig. 4(b), we plot the value of $I_{bs} = \mathrm{ZBC_{core}} - 1$, which is proportional to the strength of bound states ($\mathrm{ZBC_{core}}$ is the normalized ZBC measured at core center, and $I_{bs} = 0$ corresponds to the disappearance of core states). It is clear that I_{bs} exponentially drops to zero for $B > 0.4$ T. All these anomalous behaviors usually are not expected for type-II superconductors. Actually they imply strong overlapping happened between vortices at low field. The shrinkage of vortex core is a direct consequence of vortex overlapping, and the suppression of core bound states is due to the weakening of the surrounding superconducting gap (the potential barrier), which can no longer confine the quasiparticles. Based upon these observations, below we argue that the whole physical picture here can be explained by multiband superconductivity. As shown in band calculations, $Ta_4Pd_3Te_{16}$ has four bands (two 1D-like, one 2D-like, and one 3D-like) across E_F [9]. Here the tunneling direction is kept perpendicular to the cleaving plane, the tunneling probabilities of different bands will depend on their specific band structure and orbital characters, which could be very different [18]. (Considering the 3D band might have larger tunneling probabilities than the in-plane 2D bands and larger DOS at E_F as calculated in Ref. [9], one may expect the measured superconducting gap is mainly from the 3D band). As indicated by the large vortex size in Fig. 3(a), the observed superconducting gap may not be the one that dominates bulk H_{c2}. (The disappearance of the gap at 1.5 T is a further evidence.) So it is very likely that there exists a "hidden" band which has a larger superconducting gap and much shorter coherence length. This band dominates the bulk superconductivity of $Ta_4Pd_3Te_{16}$, but it has a small tunneling probability so it is overwhelmed by other bands in tunneling conductance. In very low field (compared to H_{c2}), the forming of vortices is dominated by the observed gap with long coherence length (reflected by the large core size). When the field increases, the superconductivity of the observed band will be suppressed faster than that of the "hidden" band. The suppression is manifested through strong vortex overlapping, which causes the shrinkage of cores size and the fast closing of the superconducting gap in regions outside the vortices. In other words, the whole system will have a field dependent coherence length. Actually similar behaviors have been observed in the well-known multiband superconductors MgB_2 and $NbSe_2$ [17–24]. But here further calculation is needed to clarify each band contribution to the total tunneling conductance.

Because of vortex overlapping Eq. (1) is no longer valid for ξ estimation. To quantitatively describe the core size, we measured the full width at half maximum [FWHM, as marked in Fig. 3(i)] of the ZBC line cut through vortex cores (along the long and short axes) and plot their field dependence in Fig. 4(c). We also simulated vortex mappings by arranging the cores [with the size fitted from Fig. 3(a)] into the lattices extracted from Figs. 3(a)–3(h). (Note that the vortex lattice symmetry also changes with field. The lattice is elongated along the stripe direction for $B < 0.7$ T, but became nearly sixfold symmetric for $B > 1.0$ T.) The simulated mappings are shown in Fig. 5. The FWHMs extracted from the simulations are ploted in Fig. 4(c) (solid curves). One can see the calculated curves fit the data at low field region but deviate at higher fields. This may be due to the fact that in a multiband system there always exists interband couplings, thus a field-dependent coherence length (as reported for $NbSe_2$ and MgB_2 [21–23]) will be more preferable to describe the system. However, due to the absence of the "hidden" bands in our data, we cannot extract the real coherence length of the system from the mappings directly. In Fig. 4(c) one can see the anisotropy of vortex cores decreases as the field increases (the ratio of the long-axis length to the short-axis length changes from 2.9 at 0.05 T to 2.0 at 1.2 T). This together with the lattice symmetry changing may also be due to interband coupling, and imply the "hidden" band is more

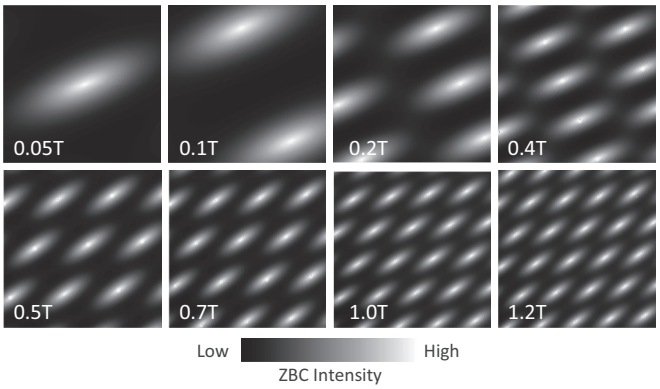

FIG. 5. Simulated vortex mappings at various field (marked on each image) by using the vortex overlapping model (see text).

isotropic than the observed band. Because it is well known the vortex lattice symmetry is closely related to the shape of Fermi surfaces and underlying crystal lattice [25,26], and the interaction between vortices may change with magnetic field, due to the change of dominating band [27].

The suppression of core bound states [Fig. 4(b)] at rather low field indicates the delocalization of superconducting quasiparticles, which will significantly affect the transport process [19,28]. Indeed the field dependence of thermal conductance of $Ta_4Pd_3Te_{16}$ shows an upturn at the low field region [8]. This is fully consistent with our STM data and is a strong support of the multiband superconductivity. We also expect the field dependence of electron specific heat to be nonlinear.

At last, we discuss the electron pairing in $Ta_4Pd_3Te_{16}$. The BCS-like gap suggests a nodeless s-wave pairing symmetry. However, thermal conductivity measurements show a residual linear term at $T < 80$ mK. Since $Ta_4Pd_3Te_{16}$ is a four-band superconductor, it is possible that there exists a much smaller gap (or highly anisotropic gap) on one of the bands that we could not observe. The discrimination of these gaps will require lower temperature and different tunneling directions than the current ones. On the other hand, the observed gap of $\Delta = 0.66$ meV and $T_c = 4.3$ K produce the ratio $2\Delta/K_BT_c$ of 3.56, which is very close to the weak coupling ratio. But as discussed it should be a "hidden" band(s) that dominates the bulk superconductivity, which has a larger gap and consequently gives a larger ratio. In addition, the observed CDW-like modulations imply strong electron-phonon couplings in the system. Therefore, $Ta_4Pd_3Te_{16}$ may be a strongly coupled superconductor. The relationship between CDW and superconductivity in such a quasi-1D system is intriguing and calls for further study.

In summary, we investigated the quasi-1D superconductor $Ta_4Pd_3Te_{16}$ by low temperature STM/STS. We observed CDW-like modulations along the atomic chains and BCS-like superconducting gap. The highly anisotropic vortex manifests its quasi-1D electronic structure. The anomalous field dependence of the vortex core size, rapid suppression of the superconducting gap, and the core bound states indicate that $Ta_4Pd_3Te_{16}$ is a multiband superconductor. Our results suggest that $Ta_4Pd_3Te_{16}$ is an interesting playground for studying CDW and multiband superconductivity.

Note added in proof. Upon finishing this work, we noticed a similar independent study by Z. Du *et al.* posted in arXiv:1412.3993.

We thank Shiyan Li and Jiangping Hu for useful discussions. This work is supported by the National Science Foundation of China, and the National Basic Research Program of China (973 Program) under Grant No. 2012CB921402, No. 2011CBA00112, and No. 2011CB921802.

[1] J. G. Bednorz and K. A. Müller, Z. Phys. B **10**, 189 (1986).
[2] Y. Kamihara, T. Watanable, M. Hirano, and H. Hosono, J. Am. Chem. Soc. **130**, 3296 (2008).
[3] C. Petrovic, P. G. Pagliuso, M. F. Hundley, R. Movshovich, J. L. Sarrao, J. D. Thompson, Z. Fisk, and P. Monthoux, J. Phys.: Condens. Matter **13**, L337 (2001).
[4] D. Jérome, A. Mazaud, M. Ribault, and K. Bechgaard, J. Phys. Lett. **41**, L95 (1980).
[5] K. Bechgaard, K. Carneiro, M. Olsen, F. B. Rasmussen, and C. S. Jacobsen, Phys. Rev. Lett. **46**, 852 (1981).
[6] W. H. McCarroll and M. Greenblatt, J. Solid State Chem. **54**, 282 (1984).
[7] W. H. Jiao, Z. T. Tang, Y. L. Sun, Y. Liu, Q. Tao, C. M. Feng, Y. W. Zeng, Z. A. Xu, and G. H. Cao, J. Am. Chem. Soc. **136**, 1284 (2014).
[8] J. Pan, W. H. Jiao, X. C. Hong, Z. Zhang, L. P. He, P. L. Cai, J. Zhang, G. H. Cao, and S. Y. Li, arXiv:1404.0371.
[9] D. J. Singh, Phys. Rev. B **90**, 144501 (2014).
[10] P. Alemany, S. Jobic, R. Brec, and E. Canadell, Inorg. Chem. **36**, 5050 (1997).
[11] A. Mar and J. A. Ibers, J. Chem. Soc., Dalton Trans. 639 (1991).
[12] Z. Z. Wang, J. C. Girard, C. Pasquier, D. Jérome, and K. Bechgaard, Phys. Rev. B **67**, 121401 (2003).
[13] C. Brun, Z. Z. Wang, and P. Monceau, Phys. Rev. B **80**, 045423 (2009).
[14] H. F. Hess, R. B. Robinson, R. C. Dynes, J. M. Valles, Jr., and J. V. Waszczak, Phys. Rev. Lett. **62**, 214 (1989).
[15] F. Gygi and M. Schlüter, Phys. Rev. B **43**, 7609 (1991).
[16] M. Zehetmayer, Supercond. Sci. Technol. **26**, 043001 (2013).
[17] M. R. Eskildsen, M. Kugler, S. Tanaka, J. Jun, S. M. Kazakov, J. Karpinski, and Ø. Fischer, Phys. Rev. Lett. **89**, 187003 (2002).
[18] A. Brinkman, A. A. Golubov, H. Rogalla, O. V. Dolgov, J. Kortus, Y. Kong, O. Jepsen, and O. K. Andersen, Phys. Rev. B **65**, 180517 (2002).
[19] F. Bouquet, Y. Wang, I. Sheikin, T. Plackowski, A. Junod, S. Lee, and S. Tajima, Phys. Rev. Lett. **89**, 257001 (2002).
[20] N. Nakai, M. Ichioka, and K. Machida, J. Phys. Soc. Jpn. **71**, 23 (2002).
[21] F. D. Callaghan, M. Laulajainen, C. V. Kaiser, and J. E. Sonier, Phys. Rev. Lett. **95**, 197001 (2005).
[22] M. Eisterer, M. Zehetmayer, H. W. Weber, and J. Karpinski, Phys. Rev. B **72**, 134525 (2005).
[23] T. Klein, L. Lyard, J. Marcus, Z. Holanova, and C. Marcenat, Phys. Rev. B **73**, 184513 (2006).
[24] Y. Noat, T. Cren, F. Debontridder, D. Roditchev, W. Sacks, P. Toulemonde, and A. San Miguel, Phys. Rev. B **82**, 014531 (2010).
[25] M. R. Eskildsen, P. L. Gammel, B. P. Barber, U. Yaron, A. P. Ramirez, D. A. Huse, D. J. Bishop, C. Bolle, C. M. Lieber, S. Oxx, S. Sridhar, N. H. Andersen, K. Mortensen, and P. C. Canfield, Phys. Rev. Lett. **78**, 1968 (1997).
[26] V. G. Kogan, M. Bullock, B. Harmon, P. Miranovic, Lj. Dobrosavljevic-Grujic, P. L. Gammel, and D. J. Bishop, Phys. Rev. B **55**, R8693 (1997).
[27] Victor Moshchalkov, Mariela Menghini, T. Nishio, Q. H. Chen, A. V. Silhanek, V. H. Dao, L. F. Chibotaru, N. D. Zhigadlo, and J. Karpinski, Phys. Rev. Lett. **102**, 117001 (2009).
[28] Etienne Boaknin, M. A. Tanatar, Johnpierre Paglione, D. Hawthorn, F. Ronning, R. W. Hill, M. Sutherland, Louis Taillefer, Jeff Sonier, S. M. Hayden, and J. W. Brill, Phys. Rev. Lett. **90**, 117003 (2003).